

EXPERIMENTAL/NUMERICAL ACOUSTIC CORRELATION OF HELICOPTER UNSTEADY MANOEUVRES

Massimo Gennaretti[§], Giovanni Bernardini[§], Sander Hartjes[†]
Alessandro Scandroglio^{*}, Luca Riviello^{*}, Enrico Paolone^{*}

[§]Dept. of Engineering, Roma Tre University, Rome, Italy

[†]Dept. of Aerospace Engineering, Delft University of Technology, Delft, The Netherlands

^{*}Leonardo Helicopters, Cascina Costa, Italy

Abstract

This paper presents one of the main objective of WP1 of Clean Sky GRC5 MANOEUVRES project, which consists in the correlation of ground noise data measured during flight tests, with numerical predictions obtained by a numerical process aimed at the analysis of the acoustic field emitted by helicopter rotors in arbitrary unsteady manoeuvring flight. Two of the helicopter trajectories analysed by the dedicated GRC5 flight test campaign are considered. Noise measurements obtained by microphones located on the ground at several positions along and aside the ground projection of the vehicle fly-over trajectory are used for correlation. The numerical simulation starts with the aeromechanic identification of the flown trajectory, followed by the corresponding prediction of aerodynamic loads, rotor noise radiation and far field atmospheric propagation.

1. INTRODUCTION

One of the main factors that limit public acceptance of rotorcraft is the noise emitted over densely populated areas, which prevents a wider diffusion of these vehicles capable of performing flight operations otherwise unattainable. It is the result of complex phenomena generated aerodynamically by main and tail rotors, and mechanically by engine and transmission system. Significant research effort is currently made for reducing rotorcraft acoustic impact, both by helicopter manufacturers and by research institutes and academia.

In this framework, observing that this problem is particularly relevant for operations in proximity to the ground (like, for instance, in approach and departure procedures), the Clean Sky GRC5 MANOEUVRES project^[1,2] aims at the demonstration of the feasibility of an innovative methodology to noise abatement in rotorcraft terminal manoeuvres, based on in-flight monitoring of the emitted acoustic annoyance. The MANOEUVRES in-flight noise monitoring system delivers a new cockpit instrument, the Pilot Acoustic Indicator (PAI), which conveys noise information to the pilot, allowing him/her to react adequately in case of nearing admissible noise thresholds. The PAI is fed by a quasi-steady noise estimation algorithm which provides the real-time measure of the acoustic impact. It exploits

a database of sound levels distributions over a hemisphere surrounding the vehicle, evaluated off-line for a suited set of steady operating conditions, parametrized with advance ratio, rotor thrust coefficient, and main rotor tip-path-plane angle of attack.^[2]

Within one of the workpackages of MANOEUVRES (namely, WP1), the accuracy of noise predictions provided by two different quasi-steady acoustic techniques candidate for application in the PAI tool has been assessed by comparison with a fully unsteady simulation methodology, and the corresponding results have been recently presented in Refs. [3,4]. As a follow-up of that paper, here the outcomes of the activity developed for completion of WP1 of the project MANOEUVRES are presented. Specifically, it concerns the correlation of the acoustic disturbance predicted by a computational approach based on the fully unsteady aeroacoustic formulation presented in Refs. [3,4], with that measured in the flight test campaigns performed by the GRC5 consortium.^[1] The acoustic disturbance is given in terms of noise footprints related to a set of approaching flight paths suitably prescribed.

The computation of the noise on the ground is evaluated by a two-step procedure: first, aeroacoustic maps on hemispheres rigidly connected to the helicopter are evaluated for a discrete number of finite time intervals

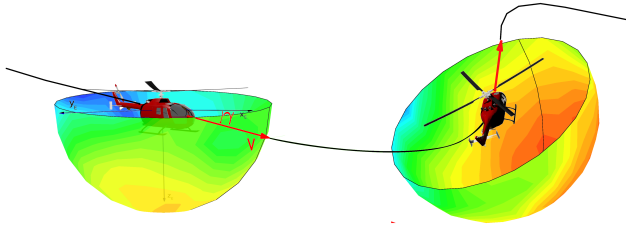


Figure 1: Noise hemisphere concept.

along the trajectory by the fully unsteady aeroacoustic methodology, and then the noise is radiated from the hemispheres to the ground through a propagation algorithm taking into account atmospheric and terrain sound attenuation/distortion effects.^[5] Note that, the noise unsteady simulation technique requires the sequential application of an aeromechanics solver for flight condition identification, an aerodynamics tool for blade loads evaluation, and an aeroacoustic solver for the near field noise prediction. This aeroacoustic simulation approach has already been applied in Refs. [3, 4] for the comparison among the hemisphere noise predictions provided by the fully unsteady aeroacoustic solver and the quasi-steady techniques examined in that work.

In this paper, the noise measurements taken in the flight test campaign are presented and correlated with the aeroacoustic unsteady simulations, in order to assess the quality of the numerical predictions considered in the MANOEUVRES project, and hence of the PAI noise estimation algorithm.

2. NOISE PREDICTION TECHNIQUE

As already mentioned in the Introduction, the noise prediction technique applied in this paper requires the sequential application of four solution tools: (i) an aeromechanics solver for the identification of the helicopter flight conditions corresponding to a given manoeuvre (namely, time histories of pilot commands, centre of mass trajectory and velocity, helicopter orientation), (ii) a rotor aerodynamics solver^[6] that, for given flight conditions, provides the associated blade airloads, (iii) a compact-source aeroacoustic solver^[7,8] based on the Farassat Formulation 1A^[9] that determines the noise hemisphere starting from the distributed blade airloads (see Fig. 1), and finally (iv) a far-field noise propagation tool taking into account atmospheric and terrain sound attenuation/distortion effects.^[5]

Aeroacoustics, aeromechanics and aerodynamics prediction tools applied in this work are briefly described in

the next sections.

3. AEROMECHANICS AND AERODYNAMICS PREDICTION TOOLS

To support the specific aeromechanics analyses required by the project MANOEUVRES, Leonardo Helicopters (LH, formerly AgustaWestland) makes use of its reference company tools for flight dynamics and aerodynamics simulation: here, these are run in a loosely coupled and modular fashion, to segregate and simplify the solution process and allow parallelization of the technical activities. In practice, first, the flight mechanics software uses a simplified modelling approach for blade dynamics and aerodynamics, to simulate the trimmed conditions, as well as the fully unsteady response of the vehicle, and then, the computed flight parameters are used as inputs to the aerodynamic solver. The aerodynamic simulation is determined by matching the pilot controls, the vehicle flight mechanics states and the main and tail rotor hub generalized forces (and therefore the advance ratio, rotor thrust coefficient, and rotor tip-path-plane angle of attack) as previously calculated in the flight dynamics analysis phase.

3.1. Aeromechanics simulation

Whenever applicable, the flight mechanics simulation of unsteady flight is performed using a manoeuvre tracking technique: similarly to what a pilot would do with the actual vehicle, a set of synthetic autopilot control logics is applied to steer the vehicle virtual model along the desired flight path, either coming from flight tests or designed for the purpose of the prediction task. The autopilot method, well known in the past for helicopter trim simulations, has been effectively applied in past European research efforts (for instance in the software EUROPA used in projects like RESPECT and NICETRIP) and is here implemented in a multi-layer set of generalized control logics, called APHELION.

Note that, as the vehicle considered in the project is a legacy company helicopter with no major configuration changes, the rotorcraft software models employed are extremely accurate and reliable, in that based on past extensive investigations and validations on quite large flight regime envelopes.

One of the key features of the working process described above is that it allows the very efficient use of state-of-the-art methods for each discipline, assuming that the interfaces and the iterations on the computed results are rigorously and transparently defined and performed. For instance, the same flight simula-

tion software, Flightlab[®] by Advanced Rotorcraft Technology Inc. (ART), can be used in this research in all tasks, from the simple trim calculation to the unsteady simulation of entire flight procedures, or even to piloted simulation trials in the LH Engineering Simulator facility. Flightlab[®] allows users to apply high-fidelity simulation models by arbitrarily selecting from a library of modelling components, interconnecting them into a custom architecture, and assigning aircraft specific data to the parameters of these components.

This flexibility is used here to run the same real-time capable helicopter model with few rotor blade dynamics states, nonlinear compact rotor wake models (Peters-He dynamic wake model), nonlinear modelling of static aerodynamics and flight controls in any flight condition examined, and to connect turboshaft engine, engine control system and flight control system models, for example, only when necessary. Recently, Flightlab[®] has been one of the main tools applied for the development of the ERICA tiltrotor concept in European research programs like NICETRIP, and is adopted by LH in most of its current design, development and certification activities.

3.2. Aerodynamics simulation

The aerodynamic blade loading required by the acoustic code, is obtained by means of the LH in house ADPANEL solver.^[6] ADPANEL is a full-unstructured panel code implementing the most advanced aerodynamic features in the field of potential methods. It is capable to represent body surfaces in unstructured-hybrid meshes, while the wake representation is based on the Constant Vorticity Contour (CVC) modelling of both rotary and fixed wing. More in detail, Dirichlet approach was chosen in ADPANEL, since it was found to be more robust and computationally efficient. The wake model implemented in ADPANEL is composed by two parts: the dipole buffer wake sheet and a set of Constant Vorticity Contour (CVC) vortex filaments. This dipole is generated every time step and is converted, after the resolution of the Laplace equation, in CVC vortex filaments (see Fig. 2); before the conversion, starting from the second time iteration, an equivalent vortex is generated along the confinement of the buffer region in order to erase the not-balanced amount of circulation while difference in time generates the first shed vortex. Kutta Condition is used to prescribe the stream-wise vorticity released both by wings and rotor blades. Finally a Multi-Block (Iterative) & Accelerated Flow Solver based on a Multi-Processor Implementation (MPI) maximize the ADPANEL computational efficiency.

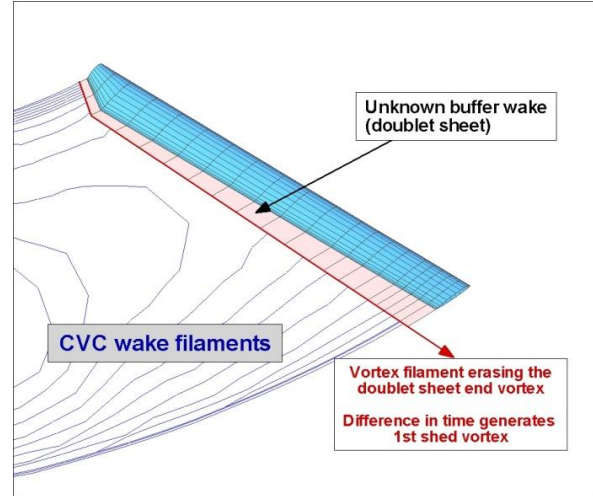


Figure 2: Wake modelling in ADPANEL.

The peculiarity of its formulation makes ADPANEL suitable to treat complex fully unsteady problems. It provides aerodynamic simulations through a time marching, unsteady solution scheme: suitable input flight parameters are considered for examining simplified problems like, for instance, wings in steady, rectilinear flight.

Within this work, a fully coupled main rotor and tail rotor simulation is applied in order to take into account the interactions between the main rotor wake with the tail rotor blades: based on LH experience, this type of aerodynamic simulation is the most reliable for acoustic predictions.

4. NOISE PROPAGATION PREDICTION TOOLS

Noise radiated by helicopter rotor blades is evaluated through solution of the well-known Ffowcs Williams and Hawkings equation,^[10] which governs the propagation of acoustic disturbances aerodynamically generated by moving bodies.

The boundary integral formulation developed by Farassat known as Formulation 1A^[9] is a widely-used, computationally efficient way to determine solutions of the Ffowcs Williams and Hawkings equation, and is particularly suited for the problems examined here. When the velocity of the rotor blades is far from the transonic/supersonic range, it yields the aeroacoustic field as a superposition of two terms, both expressed by integrals evaluated over the actual blade surface, S_B :^[9] the loading noise, p'_L , related to the distribution of pres-

sure over blade surfaces

$$(1) \quad 4\pi p'_L(\mathbf{x}, t) = \frac{1}{c_0} \int_{S_B} \left[\frac{\dot{\tilde{p}} \mathbf{n} \cdot \hat{\mathbf{r}} + \tilde{p} \dot{\mathbf{n}} \cdot \hat{\mathbf{r}}}{r|1 - M_r|^2} \right]_\tau dS(\mathbf{y}) \\ + \int_{S_B} \left[\frac{\tilde{p} \mathbf{n} \cdot \hat{\mathbf{r}} - \tilde{p} \mathbf{M} \cdot \mathbf{n}}{r^2|1 - M_r|^2} \right]_\tau dS(\mathbf{y}) \\ + \frac{1}{c_0} \int_{S_B} \left[\frac{\tilde{p} \mathbf{n} \cdot \hat{\mathbf{r}}}{r^2|1 - M_r|^3} r \dot{\mathbf{M}} \cdot \hat{\mathbf{r}} \right]_\tau dS(\mathbf{y}) \\ + \int_{S_B} \left[\frac{\tilde{p} \mathbf{n} \cdot \hat{\mathbf{r}}}{r^2|1 - M_r|^3} (M_r - M^2) \right]_\tau dS(\mathbf{y})$$

and the thickness noise, p'_T , that depends on blade geometry and kinematics

$$(2) \quad 4\pi p'_T(\mathbf{x}, t) = \int_{S_B} \left[\frac{\rho_0 \dot{v}_n}{r|1 - M_r|^2} \right]_\tau dS(\mathbf{y}) \\ + \int_{S_B} \left[\frac{\rho_0 v_n (r \dot{\mathbf{M}} \cdot \hat{\mathbf{r}} + c_0 M_r - c_0 M^2)}{r^2|1 - M_r|^3} \right]_\tau dS(\mathbf{y})$$

In the equations above, r denotes the distance between observer position, \mathbf{x} , and source position, \mathbf{y} , whereas $\hat{\mathbf{r}} = \mathbf{r}/r$ is the unit vector along the source-observer direction, with $r = |\mathbf{r}|$. In addition, c_0 and ρ_0 are the speed of sound and the density in the undisturbed medium, respectively, $\tilde{p} = (p - p_0)$ with p_0 representing the undisturbed medium pressure, $\mathbf{M} = \mathbf{v}_B/c_0$ with \mathbf{v}_B denoting the body velocity, $M = \|\mathbf{M}\|$, $M_r = \mathbf{M} \cdot \hat{\mathbf{r}}$, and $v_n = \mathbf{v}_B \cdot \mathbf{n}$, where \mathbf{n} is the outward blade surface unit normal vector. Further, \dot{v}_n , $\dot{\mathbf{n}}$ and $\dot{\mathbf{M}}$ denote time derivatives of v_n , \mathbf{n} and \mathbf{M} , observed in a frame of reference fixed with the undisturbed medium. The notation $[\dots]_\tau$ indicates that all quantities must be evaluated at the emission time τ , *i.e.*, the time at which the signal arriving in \mathbf{x} at time t started from $\mathbf{y} \in S_B$.^[9]

In problems dealing with weakly loaded rotors, thickness and loading noise are comparable. However, when strongly loaded rotors are examined, thickness noise contribution tends to be negligible and the acoustic disturbance is dominated by loading noise. Thus, from Eq. (1) it is apparent that for accurate noise simulation, accurate simulation of blade airloads is required.

Commonly, applications of aeroacoustic formulations for helicopter rotor analysis consider steady, rectilinear, trimmed flights. In these operative conditions both kinematics and aerodynamics are periodic thus yielding, correspondingly, periodic integrand functions, periodic kernels and, for observers rigidly connected to a helicopter-fixed frame of reference, periodic delays as well (it is worth noting that the periodicity occurs in coordinated turns).

Differently, during unsteady helicopter manoeuvres kinematic and aerodynamic terms are non-periodic, thus increasing the complexity of the algorithms to be applied for implementing Eqs. (1) and (2). Time delays, θ , appearing in thickness and loading noise expressions are obtained as solutions of a root-finding problem for the following nonlinear equation

$$\|\mathbf{x}(t) - \mathbf{y}(t - \theta)\| = c_0 \theta$$

and thus, the prediction of radiated noise requires the knowledge of the past time histories of blade pressure loads and vehicle and blade kinematics, for a time interval length depending on observer location. Indeed, time histories of center of mass trajectory and velocity, vehicle attitude and angular velocity are necessary data to evaluate instantaneous values of kernels and integral coefficients of the discretized versions of Eqs. (1) and (2).

4.1. Compact-Source Aeroacoustic Formulation

In order to optimize the computational performance of the aeroacoustic solver presented in the previous section, while limiting, at the same time, the amount of data exchange from aerodynamic to aeroacoustic solvers (a particularly relevant issue in noise predictions concerning rotorcraft manoeuvring flights), the so-called compact source versions of it could be conveniently applied. Those introduced in the last decade are based on the knowledge of spanwise distribution of sectional lift;^[11,12] they provide satisfactorily accurate noise predictions when pressure distribution presents limited values of chordwise gradient, and are applicable by using blade loads predicted by aerodynamic models typically considered in rotorcraft comprehensive codes.^[13]

Starting from the Farassat 1A Formulation, the compact form of the loading noise term, p'_L , reads^[7,8,11]

$$(3) \quad 4\pi p'_L(\mathbf{x}, t) = \frac{1}{c_0} \int_0^R \left[\frac{\dot{\mathbf{L}} \cdot \hat{\mathbf{r}}}{r|1 - M_r|^2} \right]_\tau d\ell(\mathbf{y}) \\ + \int_0^R \left[\frac{\mathbf{L} \cdot (\hat{\mathbf{r}} - \mathbf{M})}{r^2|1 - M_r|^2} \right]_\tau d\ell(\mathbf{y}) \\ + \frac{1}{c_0} \int_0^R \left[\frac{\mathbf{L} \cdot \hat{\mathbf{r}} (r \dot{\mathbf{M}} \cdot \hat{\mathbf{r}} + c_0 M_r - c_0 M^2)}{r^2|1 - M_r|^3} \right]_\tau d\ell(\mathbf{y})$$

where R is the blade radius and, in this case, r denotes the distance between the observer point, \mathbf{x} , and the compacted source point, \mathbf{y} , located along the blade

span. In addition,

$$\mathbf{L} = - \int_{LE}^{TE} \Delta p \mathbf{n} ds$$

is the section force vector, with \mathbf{n} and p denoting upward unit normal to airfoil mean-line and pressure jump, respectively.

The compact-source integral representation in Eq. 3 is applicable when the chord length is negligible with respect to the source-observer distance, r , and predicts the same radiated sound for any chordwise pressure distributions providing the same spanwise distribution of sectional forces, \mathbf{L} .

4.2. Atmospheric Noise Propagation Algorithm

The propagation losses between source and receiver, and the resulting noise exposure on the ground are determined through a three-step process.^[5]

Firstly, the path of the sound ray between the helicopter and a ground-based receiver is determined. Rather than using an integration over time of the ray path, a geometrical approach is used, where the atmosphere is represented as a number of layers with constant speed of sound gradients. Refraction is then accounted for within the layers rather than between the integration steps as in classical ray tracing approaches. This approach greatly reduces the number of integration steps due to the limited number of layers required, and as such allows the numerical determination of the ray paths between the source and a discrete number of receiver positions.

In the second step, the bearing between the source and the receiver and the launch angle of the sound ray at the source determines the azimuth and elevation angles where the ray passes through the hemisphere, hence providing the SPL emitted at the source. Since the ray tracing method described above is independent of the frequency, the source noise levels for all available frequencies can be determined concurrently.

With the source noise level and the ray path known, the propagation losses can be determined. The algorithm takes into account three attenuation effects: (i) atmospheric attenuation (or absorption) is accounted for using the method defined by ICAO^[14] and depends on the ray path and sound frequency; (ii) spreading loss is accounted for, which includes the effects of focusing in a refracting atmosphere;^[15] (iii) the ground effect is included using the approach defined by Delaney and Bazley,^[16] in order to account for secondary rays reflecting off different ground surface types. In addition to



Figure 3: AW139.

the three attenuation effects mentioned above, also the sound level in the shadow zone is determined. Based on the approach developed by Arntzen,^[17] the strong decrease of the sound level at the transition between the illuminated and the shadow zone is determined, as well as the noise levels penetrating the shadow zones due to ground waves, diffraction and scattering due to turbulence.

For each of the time steps available in the hemisphere samples, the total sound energy reaching the ground is determined based on the source noise levels and the propagation losses. This A-weighted sound level in each of the grid points can then be integrated over the execution time of the trajectory to obtain the Sound Exposure Level (SEL) of the full trajectory.

5. NUMERICAL RESULTS

In the following, the results of aeroacoustic correlations between numerical simulations based on the proposed solution approach and experimental measurements concerning noise emitted by the helicopter AW139 are presented.

The AW139 is a 15-seat, intermediate-class, twin-engined helicopter, with a 5-blade fully-articulated main rotor of radius $R = 6.9$ m, a 4-blade tail rotor, and maximum take-off weight of 7000 kg (see Fig. 3). First, experimental tests are described, and then the correlations are discussed.

5.1. Experimental Campaign

An experimental campaign has been accomplished to support the activities planned for WP1 of the project MANOEUVRES, aimed at acquiring measurements of the noise footprint generated by the AW139 helicopter during unsteady manoeuvres. This test campaign has been performed at the Cameri airport, and is part of the experimental activities considered within the project GRC5 Environment-Friendly Flight Paths, conceived in the framework of the wider project Clean Sky Green Rotorcraft ITD.^[18] It includes three test flights named B1(a), B1(b) and B1(c) in Ref. [18], which consist of a

deceleration in level flight, followed by an entry into descent: the deceleration is from 90 to 50 kn with airspeed gradient of (a) 1 kn/s, (b) 2 kn/s, (c) 3 kn/s, whereas the descent is kept at least for 10 seconds, along a flight path of -9 deg slope.

The noise footprint is measured through a set of microphones installed around the runway. The set-up of microphones on the ground is shown in Figs. 4 and 5, where green circles denote microphones located 1.2 m above the ground (ICAO microphones), while red circles denote ground microphones located on rigid plates at ground level.^[18]

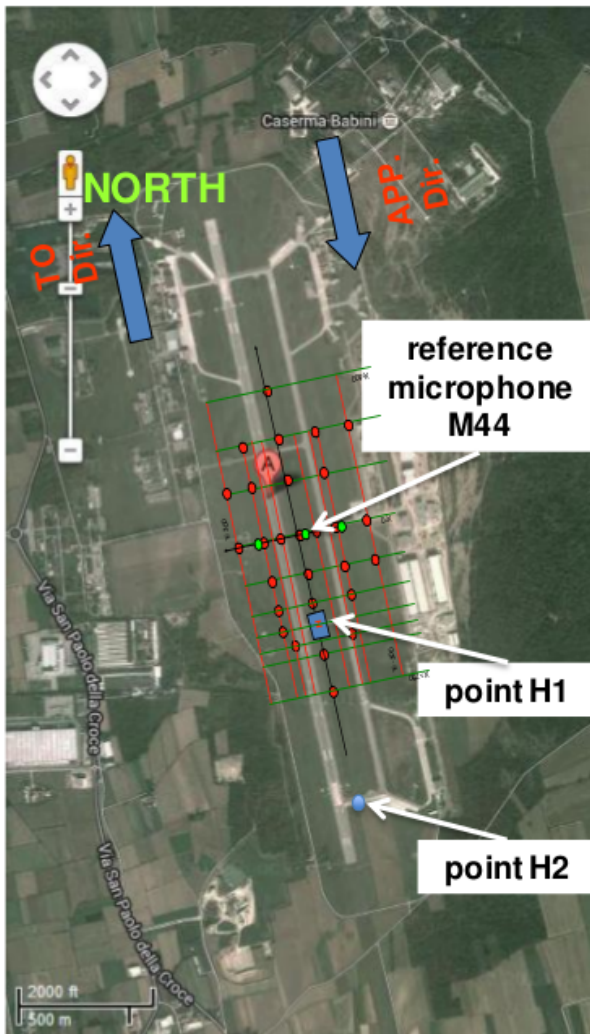


Figure 4: On-ground microphones set-up wrt runway.

For the sake of conciseness, observing that the outcomes from B1(c) are similar to those from B1(a) and B1(b), in this paper only the correlations regarding the

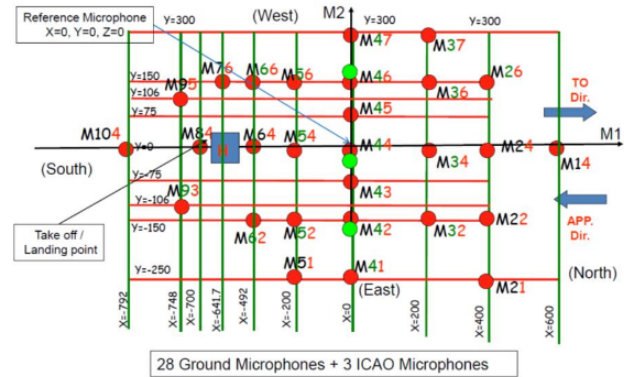


Figure 5: Details of on-ground microphones set-up.

flight tests B1(a) and B1(b) are presented and discussed.

5.1.1. Trajectory B1(a): record 23

The uniformly decelerated level flight, followed by a decelerated conversion to descent flight corresponds to the evolutions of advance ratio, μ , thrust coefficient, C_T , tip-path-plane angle of attack (TPP-AOA), α_{TPP} , path slope, γ , height, and blade pitch commands depicted in Figs. 6-11. Four flight time intervals have been selected on this trajectory (see blue segments along the curves in Figs. 6-11) for correlation of measured and numerically simulated ground noise. In the chosen intervals, different aeromechanics and aerodynamic events occur, thus producing differently generated noise emissions.

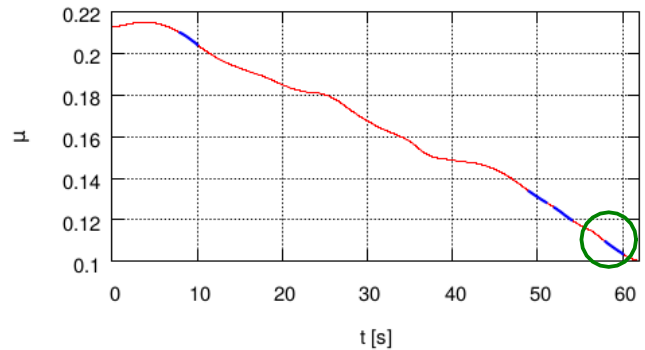


Figure 6: Advance ratio. Record 23.

5.1.2. Trajectory B1(b): Record 24

This manoeuvre corresponds to the flight parameters evolutions presented in Figs. 12-17. Five flight time intervals have been selected on this trajectory (see blue

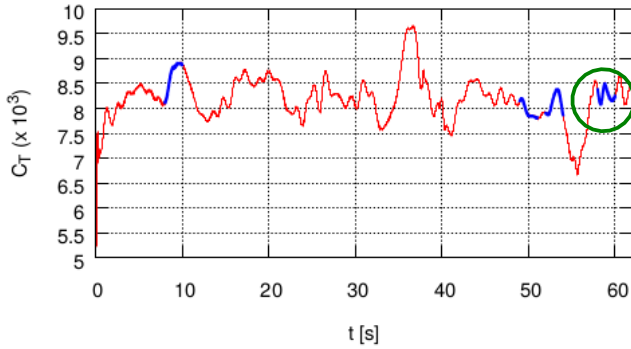


Figure 7: Thrust coefficient. Record 23.

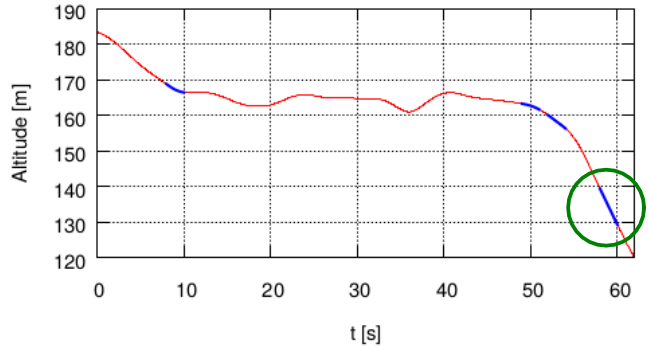


Figure 10: Altitude. Record 23.

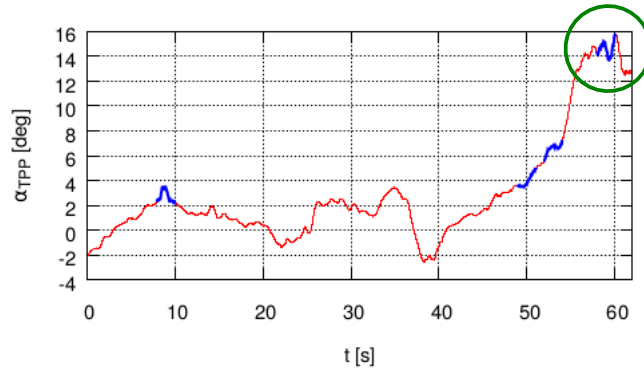


Figure 8: Main rotor TPP-AOA. Record 23.

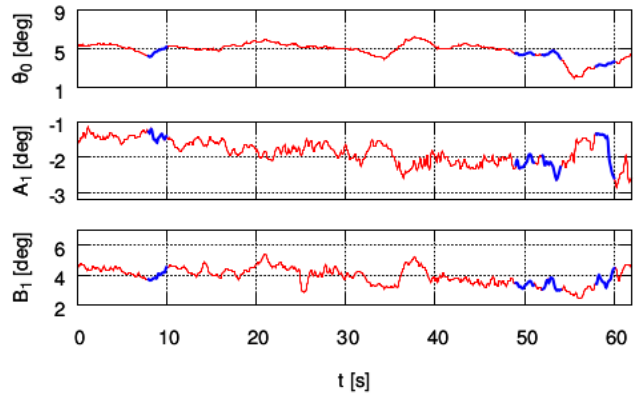


Figure 11: Main rotor blade controls. Record 23.

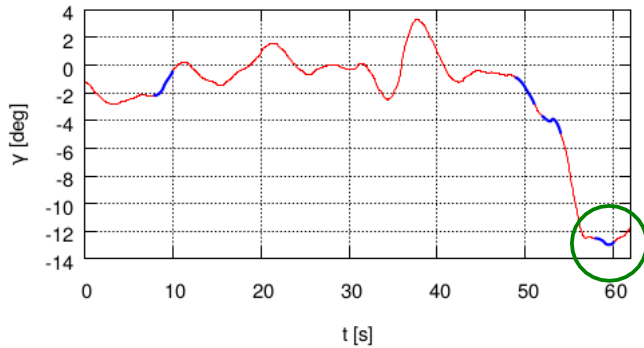


Figure 9: Flight-path angle. Record 23.

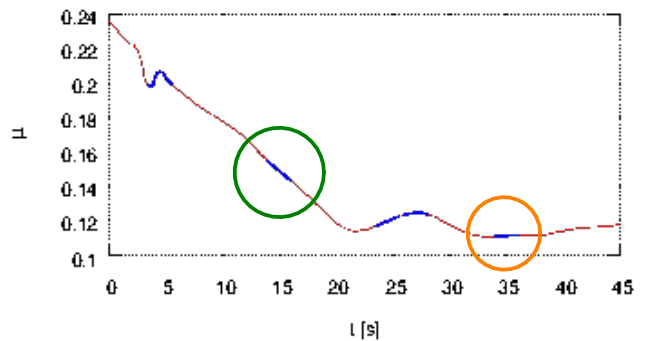


Figure 12: Advance ratio. Record 24.

segments along the curves in Figs. 12-17) for correlation of the corresponding measured and numerically simulated ground noise. Two of them are included in the uniformly decelerated level flight, other two are at the beginning and at the end of the phase of conversion to descent flight, whereas the last interval is in the middle of the uniform descent.

5.2. Measured and Simulated Ground Noise

For the trajectory segments highlighted in blue in Figs. 6-17, the noise measured at the microphones under-

lined in red in Fig. 18 is compared with that predicted by the numerical process outlined above.

It is worth noting that, the OASPL on the hemispheres from which the noise is radiated to the ground has been computed by applying a 1-rev Hanning window to avoid the onset of leakage problems (the acoustic signal from each trajectory segment is not periodic), along with a correction factor equal to 1.68 applied to the corresponding signal harmonics to compensate windowing effects on signal power. In the following, the experimen-

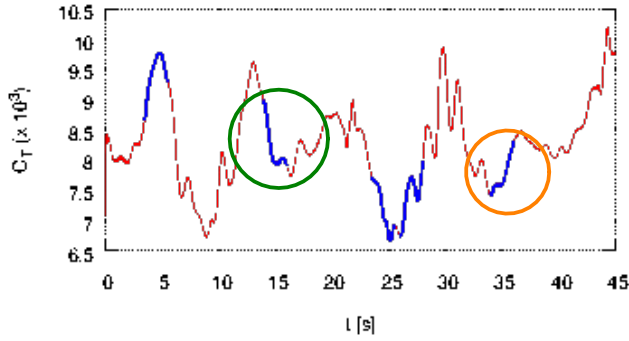


Figure 13: Thrust coefficient. Record 24.

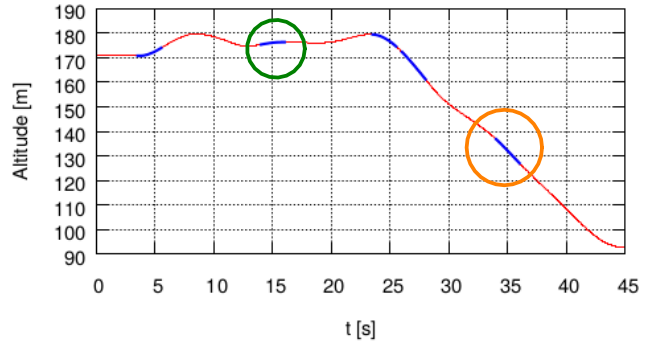


Figure 16: Altitude. Record 24.

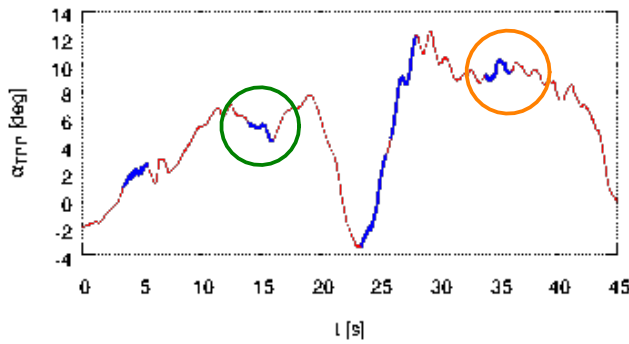


Figure 14: Main rotor TPP-AOA. Record 24.

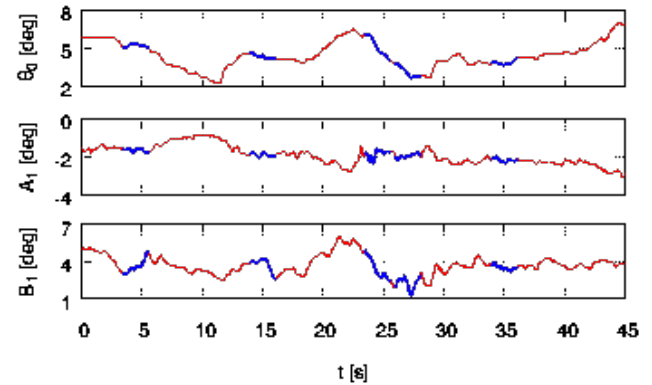


Figure 17: Main rotor blade controls. Record 24.

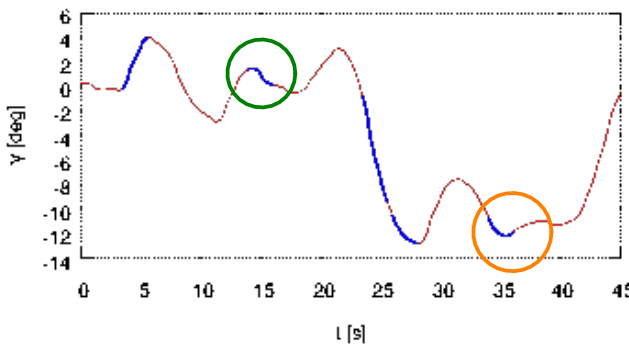


Figure 15: Flight-path angle. Record 24.



Figure 18: Examined microphones.

tal numerical correlation is presented for each trajectory examined in terms of dB_A .

5.2.1. Trajectory B1(a): Record 23

The results shown in Fig. 19 reveal that the effect of helicopter passage over the microphones is quite well captured by the predicted noise, along with the rate of attenuation due to the increase of distance. However, the instantaneous value of the predicted noise perceived at the microphone presents, sometimes, quite a relevant difference with respect to that measured experimentally. Overall, the results could be considered

moderately satisfactory.

5.2.2. Trajectory B1(b): Record 24

In this case, the results are shown in Fig. 20. Similarly to the Record 23 trajectory, the effect of helicopter passage over the microphones is quite well captured by the predicted noise, along with the rate of attenuation due to the increase of distance. In addition, the instantaneous value of the predicted noise perceived at the microphone presents, sometimes, quite a relevant difference with respect to that measured experimentally. Overall, the results could be considered mod-

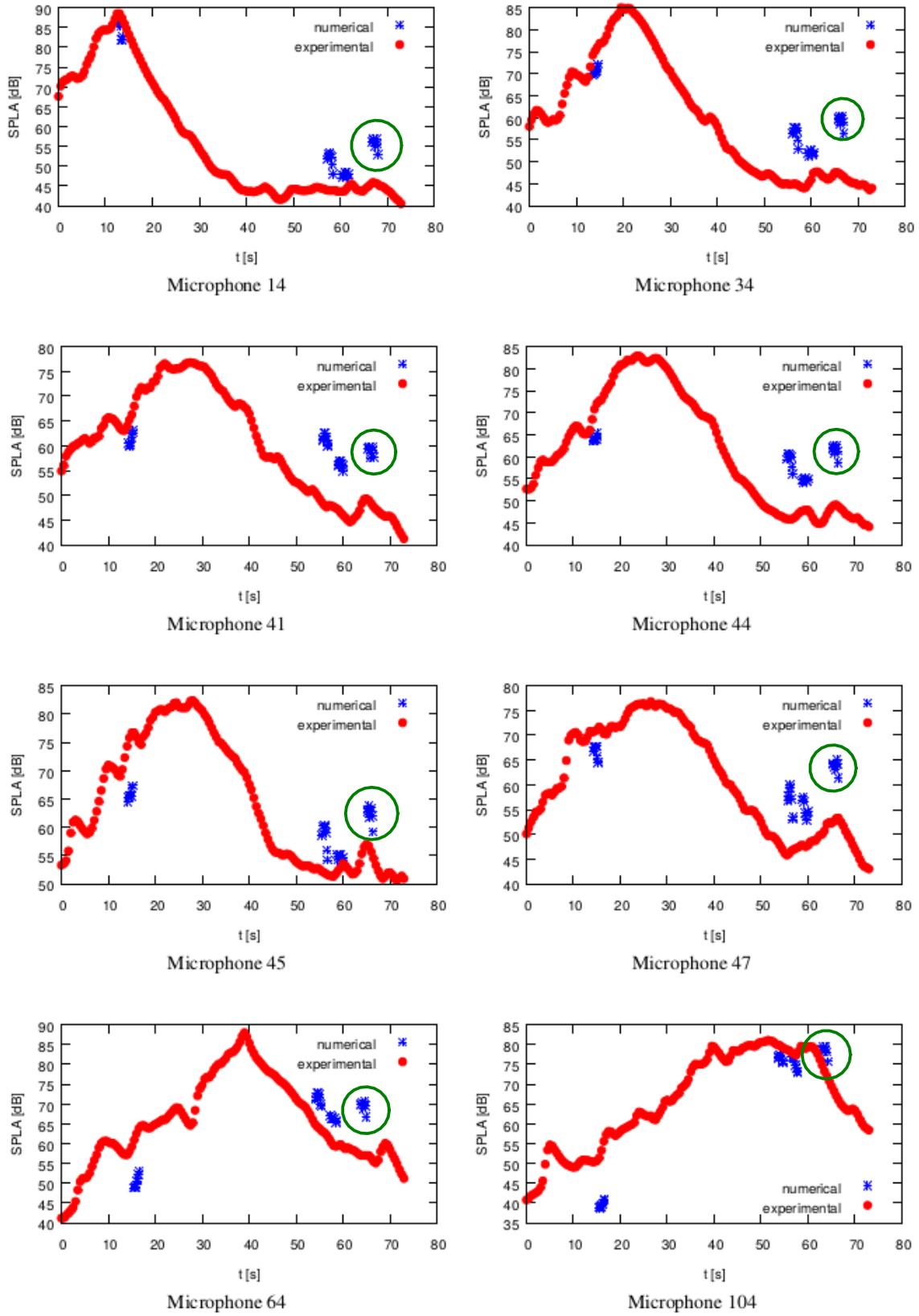


Figure 19: Experimental-numerical noise correlation for trajectory Record 23.

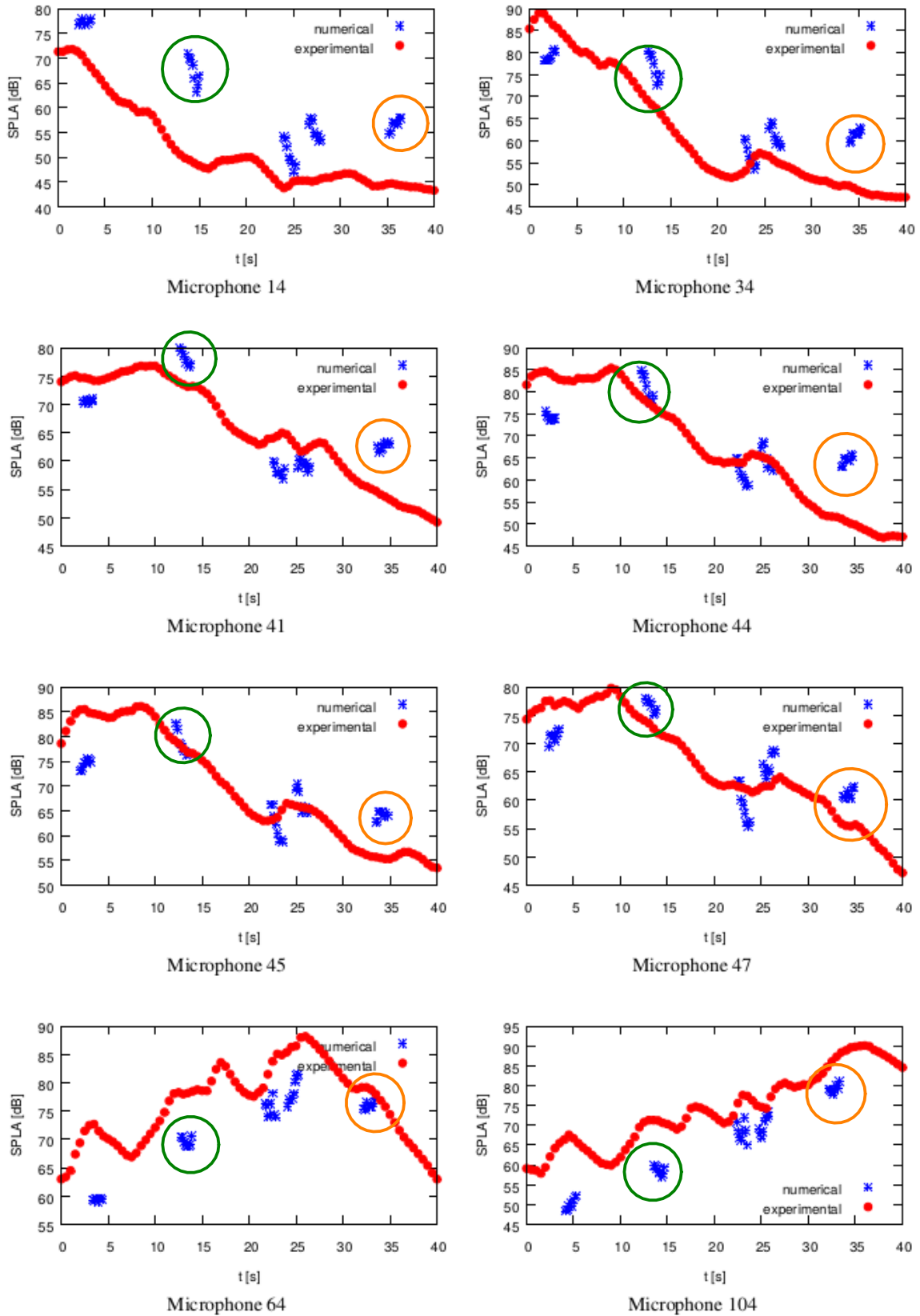


Figure 20: Experimental-numerical noise correlation for trajectory Record 24.

erately satisfactory.

5.2.3. Remarks

In order to attempt an interpretation of these globally uneven results, for each manoeuvre, in the following we compare the flight conditions which correspond to reasonably uniform speed (orange circles) and those which correspond to reasonably uniform deceleration (green circles). In the first trajectory (Record 23), a uniform speed condition is not met among the time windows considered for the computations. In the second one (Record 24) such condition can be identified in the time windows centered around $t = 35$ s.

Looking at the former case, the predictions appear systematically and significantly higher than experimental data for all microphones, except M64 and M104, where on the contrary, (more limited) underestimation occurs.

This situation is perfectly mirrored by looking at the latter case. Considering uniformly decelerated conditions, these are found in the two trajectories around $t = 65$ s and $t = 15$ s respectively (note that a time shift is present between trajectory data figures and acoustic data figures: the indicated time is referred to the time range reported in the acoustic figures). In the first case (Record 23), a higher value is systematically predicted for all microphones. The best agreement is observed for M104, where the prediction appear fairly accurate, while all other considered microphones present an almost constant difference with respect to experimental data. In the second case (Record 24), the accuracy of prediction seems to be a function of microphone position. In fact, while M14 and M34 (before M44) show high overestimation, M41 and M47 (on each side of M44) show a better, still overrating, performance, M44 and M45 (the latter very close to M44) show good results, and M64 and M104 (after M44) show significant underestimation.

Passing now to more general considerations, it can be observed that in many cases, there seems to be a general trend of underestimation during the phases in which noise more or less steadily increases. This is seen especially for microphones M64 and M104, in both trajectories. The opposite case of decreasing noise does not provide an analogous indication of a general trend, although microphones M14 and M34 seem to show constant overestimation.

6. CONCLUSIONS

The fully unsteady aeroacoustic formulation has been developed and applied. It is used to evaluate noise

hemispheres, which are the starting point for the noise propagation model taking into account atmospheric and obstacle effects. From the experimental campaign accomplished by the GRC5 Consortium two trajectories have been considered, for which several unsteady effects occurred. The ground noise has been measured on a set of microphones located around the runway at Cameri. The correlation of the noise experimental measurements with predictions corresponding to finite segments along the trajectories (selected in agreement with the GRC5 Consortium) has demonstrated that the numerical predictions:

- capture fairly well the noise-increase effect of the helicopter passage over the microphones;
- capture fairly well the rate of perceived noise attenuation due to the increase of helicopter distance;
- provide instantaneous values of the noise perceived at the microphone that often present relevant differences with respect to those measured experimentally.

Overall, the numerical noise predictions obtained by the complex fully unsteady evaluation process presented can be considered moderately satisfactory. In the next future, further correlations of numerical predictions with measured noise will be performed, in order to determine those steps in the noise evaluation process that can be improved for increasing the accuracy of the simulations. Among them, a steady, rectilinear trajectory for which the unsteady effects can be considered negligible will be analysed. In addition, different windowing of the selected trajectory time intervals examined will be applied, checking for the suitability of associated correction factors for the corresponding SPLs.

ACKNOWLEDGMENTS

The research leading to these results has received funding from Project MANOEUVRES, financed by European Community's Clean Sky Joint Undertaking Programme under Grant Agreement N. 620068.

COPYRIGHT STATEMENT

The authors confirm that they, and/or their company or organization, hold copyright on all of the original material included in this paper. The authors also confirm that they have obtained permission, from the copyright holder of any third party material included in this paper, to publish it as part of their paper. The authors confirm that they give permission, or have obtained permission

from the copyright holder of this paper, for the publication and distribution of this paper as part of the ERF proceedings or as individual offprints from the proceedings and for inclusion in a freely accessible web-based repository.

REFERENCES

- [1] Trainelli L., Gennaretti M., Zappa E., Lovera M., Rolando A., Cordisco P., Grassetti R. and Redaelli M., Development and Testing of Innovative Solutions for Helicopter In-flight Noise Monitoring and Enhanced Control Based on Rotor State Measurements. *Proc. 42nd European Rotorcraft Forum (ERF 2016)*, Lille, France, September 5-8, 2016.
- [2] Trainelli, L., Lovera, M., Rolando, A., Zappa, E., Gennaretti, M., Cordisco, P., Grassetti, R. and Redaelli, M., Project MANOEUVRES Towards Real-time Noise Monitoring and Enhanced Rotorcraft Handling Based on Rotor State Measurements. *Proc. 41st European Rotorcraft Forum (ERF 2015)*, Munich, Germany, 2015.
- [3] Gennaretti, M., Bernardini, G., Serafini, J., Trainelli, L., Rolando, A., Scandroglio, A., Riviello, L. and Paolone, E., Acoustic Prediction of Helicopter Unsteady Manoeuvres. *Proc. 41st European Rotorcraft Forum (ERF 2015)*, Munich, Germany, 2015.
- [4] Trainelli L., Gennaretti M., Bernardini G., Rolando A., Riboldi C. E. D., Redaelli M. and Riviello L., "Innovative Helicopter In-flight Noise Monitoring Enabled by Rotor State Measurements," *Noise Mapping*, Vol. 3, No. 1, 2016, pp. 190-215. doi: 10.1515/noise-2016-0014
- [5] Hartjes, S., An Optimal Control Approach to Helicopter Noise and Emissions Abatement Terminal Procedures. Ph.D. Thesis, Faculty of Aerospace Engineering, Delft University of Technology, 2015.
- [6] D'Andrea, A., Development of a Multi-processor Unstructured Panel Code Coupled with a CVC Free Wake Model for Advanced Analyses of Rotorcraft and Tiltrotors. *Proc. of American Helicopter Society 64th Annual Forum*, Montreal, Canada, 2008.
- [7] Bernardini, G., Testa, C. and Gennaretti, M., A Spectral-BEM Formulation for Compact Sources Aeroacoustics. *Proc. 21st AIAA/CEAS Aeroacoustics Conference*, Dallas, Texas, USA, 2015.
- [8] Bernardini, G., Gennaretti, M. and Testa, C., "Spectral-Boundary-Integral Compact-Source Formulation for Aero-Hydroacoustics of Rotors," *AIAA Journal*, 2016, accessed June 30, 2016. doi: <http://arc.aiaa.org/doi/abs/10.2514/1.J054923>
- [9] Farassat, F., Derivation of Formulations 1 and 1A of Farassat. *NASA TM 214853*, 2007.
- [10] Ffowcs Williams, J.E. and Hawkings, D.L., "Sound Generation by Turbulence and Surface in Arbitrary Motion," *Philosophical Transactions of the Royal Society*, London, Series A, Vol. 264, No. 1151, pp. 321-342, 1969.
- [11] Brentner, K.S. and Jones, H.E., Noise Prediction for Maneuvering Rotorcraft. AIAA Paper 20002031, *Proc. 6th AIAA/CEAS Aeroacoustics Conference*, Lahaina, Hawaii, 2000.
- [12] Brès, G.A. and Brentner, K.S., "Maneuvering Rotorcraft Noise Prediction," *Journal of Sound and Vibration*, Vol. 275, 2004, pp. 719-738.
- [13] Johnson, W., "Comprehensive Analytical Model of Rotorcraft Aerodynamics and Dynamics," Vol. I - VII, Johnson Aeronautics, September 1998.
- [14] International Civil Aviation Organization (ICAO), International Standards and Recommended Practices, Environmental Protection, Annex 16, Volume I, Aircraft Noise, Fifth Edition, (2008).
- [15] Lamancusa, J.S. and Daroux P.A., "Ray Tracing in a Moving Medium with Two-Dimensional Sound-Speed Variation and Application to Sound Propagation over Terrain Discontinuities," *Journal of the Acoustical Society of America*, Vol. 93, No. 4, 1993, pp. 1716-1726.
- [16] Delaney, M.E. and Bazley, E.N., "Acoustical Properties of Fibrous Absorbent Materials," *Applied Acoustics*, Vol. 3, No. 2, 1970, pp. 105-116.
- [17] Arntzen, M., Rizzi, S.A., Visser, H.G. and Simons, D.G., A Framework for Simulation of Aircraft Flyover Noise through a Non-Standard Atmosphere. *Proc. 18th AIAA/CEAS Aeroacoustics Conference*, Colorado Springs, CO, June 4-6, 2012.
- [18] CLEANSKY GRC5: AW139 Noise test campaign Flight test proposal, 2014.